Intelligent Structural Damage Detection with MEMS-Like Sensors Noisy Data

Intelligent structural damage detection with MEMS-like sensors noisy data

Jonathan Melchiorre[1][0000−0002−8721−8365], Laura Sardone[2][0000−0002−0928−0606] Marco Martino Rosso[1][0000−0002−9098−4132], and Angelo Aloisio[3][0000−0002−6190−0139]

[1] DISEG, Department of Structural, Geotechnical and Building Engineering, Politecnico di Torino, Corso Duca Degli Abruzzi, 24, Turin 10128, Italy; Corresponding author: marco.rosso@polito.it,

[2] DICAR, Department of Civil Engineering and Architecture Sciences, Politecnico di Bari, Via Edoardo Orabona, 4, Bari, 70126, Italy

[3] DICEAA, Department of Civil, Construction-Architecture and Environmental Engineering, Università degli Studi dell'Aquila, Piazzale Ernesto Pontieri 1, Monteluco di Roio, 67100, L'Aquila, Italy.

Abstract. In the recent period, in the civil engineering field, innovative structural health monitoring (SHM) techniques are under the spotlight, promoted by the latest developments in artificial intelligence (AI). Even just focusing on the first SHM level, i.e. the damage identification task, ground-breaking non-destructive evaluations based on output-only vibration signals have been developed lately. The current work presents two alternative methods to address an AI-based multi-class damage classification on a numerical benchmark beam problem. The main goal is to investigate the noise impacts on the simulated monitored system of micro-electro-mechanical system (MEMS) accelerometer sensors with three reasonable signal-to-noise ratio (SNR) levels. A multi-layer perceptron (MLP) neural architecture has been employed for the current task. The numerical results essentially showed that the analyzed deep learning (DL) model presents a fairly good noise immunity performance for damage detection needs with proper damage-sensitive features.

Keywords: damage detection, structural health monitoring, mems sensors, signal-to-noise ratio, multi-layer perceptron

1 Introduction

Nowadays, advanced degradation phenomena threat the safety levels of existing infrastructures [1,2,3,4,5]. Structural health monitoring (SHM) techniques have been extensively studied and developed in last decades with the final aim to monitor the health state of historical infrastructure [6,7,8,9] based on direct and indirect non-destructive testing (NDT) [10,11,12,13,14,15]. Two main approaches are used in the SHM paradigm denoted as model-driven and data-driven [16]. Moreover, input-output or output-only methods have been implemented based

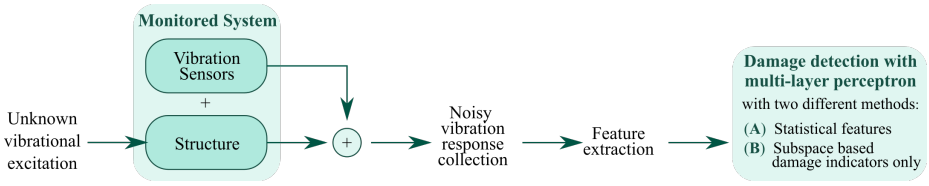

Fig. 1. Noisy vibrational structural response data collection.

on the nature of available vibration response data, further subdivided into parametric [17] and non-parametric [18] methodologies. In the current study, the output-only operational modal analysis (OMA) technique has been adopted to address the SHM first level [19], i.e. the damage identification task, aided with artificial intelligence (AI). Specifically, a neural network (NN) with a multi-layer perceptron (MLP) architecture has been used for a multi-class damage classification on a numerical benchmark beam problem. To simulate a more realistic situation, an undesired noise signal has been superimposed on the collected vibration measurements [2], representing the actual adoption of real-world micro-electro-mechanical system (MEMS) accelerometer sensors. The current study attempts to provide a novel framework for the damage detection task leveraging the potentialities of neural networks combined with output-only OMA monitoring technique, in particular with subspace-based damage indicators as damage-sensitive features. Furthermore, the main goal of the current study is to analyze the robustness of the proposed NN-based damage detection methods in presence of noisy data. Different noise levels were set by imposing a signal-to-noise ratio (SNR) [2], expressed in decibels (dB), to simulate plausible MEMS sensors.

In scientific literature, different studies have been already carried on with the adoption of NN in the SHM field. In [20], the authors analyzed the cepstrum with a NN to evaluate mass changes. In [21], flexibility matrices have been used to train deep NN obtained with OMA for near-real-time seismic damage identification. In [22], both a support vector machine model and an MLP architecture have been trained on a numerical pinned-pinned beam model to perform the damage classification task. The authors in [23], further developed the methodology proposed in [22] by also introducing a subspace-based damage indicator with statistical features, thus improving the classification accuracy. However, they trained the NN model with noise-free data. Therefore, in the current study, the authors attempted to improve the preliminary evaluations of [23] by considering more realistic noisy data.

In section 2 a brief essay on the noise levels related to the commercially available MEMS sensors for SHM is discussed. In section 3 the OMA and the adopted damage detection techniques are briefly described. In section 4, the current finite element (FE) beam model is illustrated. Finally, in section 5, the MLP model is presented and the numerical results obtained with three different noise levels have been discussed.

Table 1. Pros and cons of MEMS-WSS for SHM.

Benefits	Drawbacks	Applications
Wireless communication, onboard computation low cost, less invasive installation, small size.	Low resolution compared to wired accelerometers used in SHM application.	Nodes and platforms for autonomous data acquisition.

2 MEMS sensors noise levels

The effectiveness of an SHM procedure is strongly affected by the quality of the information retrieved from the structural system under study [2]. Despite many sources of noises actually existing [24], the vibration measurements' noise can be modeled as introduced by the sensor itself during the act of collecting the vibrational response, as depicted in Fig.1. During the last decade, SHM research moved toward innovative sensors like fiber optic, piezoelectric, and MEMS sensors, especially transitioning from wired to wireless solutions through wireless smart sensors (WSS) [25]. WSS devices are composed of nodes and platforms for autonomous data acquisition. Wireless technology has lower installation costs and allows for flexible system configurations [26]. However, battery-powered wireless sensors present still limitations related to their energy consumption, size, cost, communication range, hardware design, and risk of data loss [27]. In this study, MEMS-WSS accelerometers are considered since they are widely used in bridges SHM [28], and their main features are reported in Table 1. The overall noise level which affects the output-only vibration response signals can be quantified with the SNR. However, it does not assume a specific value for each sensor and, moreover, it is difficult to determine it in certain harsh working conditions. Nevertheless, the current state-of-the-art MEMS sensors present a SNR range between 27dB and 67dB [29]. Therefore, three different levels have been chosen to simulate MEMS in the current study: low (20dB), medium (40dB), and good (60dB) quality MEMS. An acknowledged approach in literature to simulate noisy data $y(t)$ requires superimposing a Gaussian white noise process $n(t)$ to the output-only vibrational structural response $x(t)$. The SNR can be calculated as a function of the ratio between the signal power P_{signal} and the noise power P_{noise}:

$$SNR_{dB} = 10log_{10}\left(\frac{P_{signal}}{P_{noise}}\right) \tag{1}$$

Supposing to know the SNR, the noise power is given by the inverse formula:

$$P_{noise} = \frac{P_{signal}}{10^{\frac{SNR}{10}}} \tag{2}$$

Since data are always sampled in a discrete way, the signal power is composed of discrete data amplitudes $S = \{S_1^1, S_2^1, ..., S_k^1\}$:

$$P_{signal} = \frac{1}{n}\sum_{k=1}^{n} S_k^2 \tag{3}$$

Table 2. Statistical indicators of method (A); n is the total number of time series discrete samples, $\overline{x}$ is the mean value.

Mean square: $x_{\mathrm{MS}} = \frac{1}{n}\sum_{k=1}^{n} x_k^2$	Root mean square: $x_{\mathrm{RMS}} = \sqrt{\frac{1}{n}\sum_{i=1}^{n} x_k^2}$
Variance: $x_{\mathrm{VAR}} = \frac{1}{n}\sum_{k=1}^{n} (x_k - \bar{x})^2$	Standard deviation: $x_{\mathrm{STD}} = \sqrt{\frac{1}{n}\sum_{k=1}^{n} (x_k - \bar{x})^2}$
Skewness: $x_{\mathrm{Skew}} = \frac{1}{n}\sum_{k=1}^{n} \left(\frac{x_k - \bar{x}}{x_{\mathrm{STD}}}\right)^3$	Kurtosis: $x_{\mathrm{Kurt}} = \frac{1}{n}\sum_{k=1}^{n} \left(\frac{x_k - \bar{x}}{x_{\mathrm{STD}}}\right)^4$
K-factor: $x_{\mathrm{K}} = x_{\mathrm{Max}} \cdot x_{\mathrm{RMS}}$	Maximum: $x_{\mathrm{Max}} = max\left\{\lvert x_k \rvert\right\}_{k=1}^{n}$

3 Two proposed damage detection methods for MLP

As depicted in Fig.1, in this study, the damage detection task is accomplished with a MLP deep learning (DL) architecture performing a multi-class damage classification on a numerical benchmark beam problem. After collecting vibration responses of the FE beam model under environmental excitations, the collected output-only vibration measurements have been contaminated by noise with a certain SNR to simulate real-world MEMS accelerometer sensors. Starting from these noisy data, the authors adopted a MLP classifier to distinguish vibrational samples coming from undamaged, low-damage, and severe-damage conditions. In detail, the input vector to feed the MLP $\boldsymbol{x}$ has been obtained from the feature extraction operation carried out on the noisy vibrational structural responses. The first proposed feature extraction method, denoted as (A), is based on six most informative time series statistical indicators [22]. These indicators are reported in Table 3, derived from the output-only noisy vibrational time series structural response $y(t)$. The second feature extraction method, denoted as (B), is derived from the covariance-driven stochastic subspace identification (SSI-cov) algorithm, a popular method for OMA based on the state space representation [8,30,31]. After choosing a time shift parameter, in the SSI approach, the modal information are retrieved from the singular value (SV) decomposition of the block Toeplitz matrix composed of the output covariances, denoting an active space of high values SV and a null space for almost neglectable SV. The time shift parameter governs the construction of the block Toeplitz matrix. Some scholars detected promising damage-sensitive features considering subspace residues and orthonormal properties by comparing measurements between two different

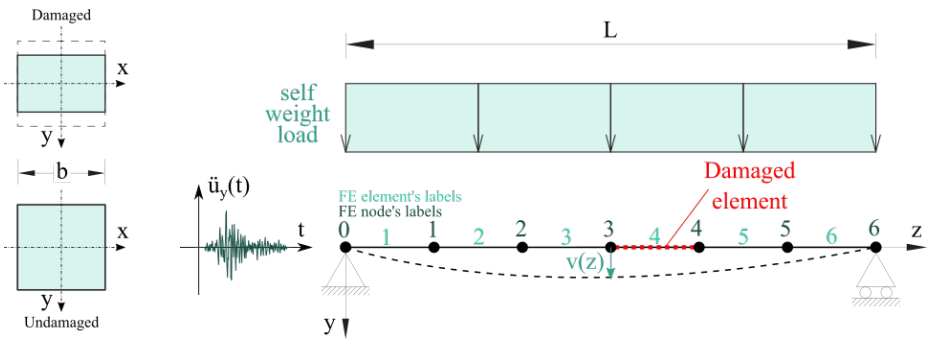

Fig. 2. FE beam model.

states, called reference and current states respectively [32]. In a nutshell, due to the orthonormal property between the two states, the matrix left product of the null space eigenvectors of the reference state with the covariance block Hankel matrix in the current state should be zero. However, due to noise, excitation variation between reference and current state, and structural damages, the resulting residues matrix seems to contain damage-sensitive information passing from zero-mean Gaussian distributed in undamaged conditions toward the non-zero mean in damaged ones. However, as it is, the residues matrix appeared not the ideal candidate for damage detection purposes because it is also influenced by noise and excitation variation. Therefore, further research demonstrated that certain parameters computed on the residues matrix may represent more valid damage-sensitive features. Yan et al. [33] presented the damage indicator (DI) of eq.(4) being the norm of residues matrix $\hat{\boldsymbol{\varepsilon}}$, which also appeared to be robust to excitation variations. The scholars also provided a geometrical interpretation of the damage indicators as the rotation angle between the two analyzed subspace states. Therefore, method (B) is based on the construction of a feature vector containing various Yan's et al. [33]. subspace-based damage indicators between the two compared reference and current state but varying the time shift parameter which governs the block Toeplitz matrix and, consequently, the block Hankel matrix.

$$DI_{\text{Yan}} = \text{norm}\,(\hat{\boldsymbol{\varepsilon}}) \tag{4}$$

4 Monitoring simulation of MEMS-like noisy data

To synthetically reproduce the noisy monitoring data coming from MEMS sensors, a numerical FE beam model has been implemented in Python OpenSeesPy environment [34]. The beam is modeled with a square cross-section of $0,10m$ and a span length of $2,00m$. Generic steel material has been implemented with Young's modulus $E = 210GPa$ and a mass density $\rho = 7850kg/m^3$. Although there are several ways to model structural damage [35,36], damaged elements have been modeled with a percentage cross-section reduction. As depicted in

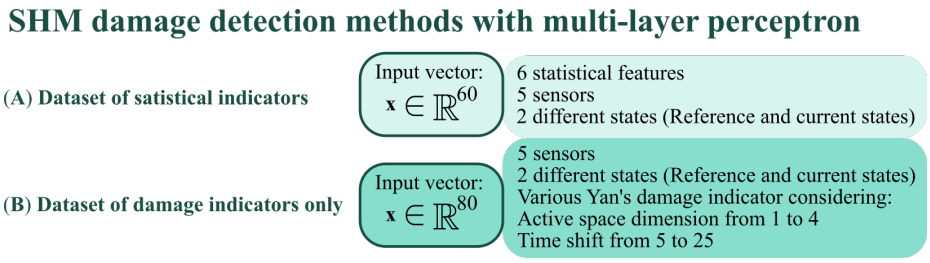

Fig. 3. Input feature vectors to the MLP network of methods (A) and (B).

Fig.2, the global coordinate system is denoted as x, y, z, b indicates the cross-section side, L the span length, g_{k1} is the self-weight which produces the static deflection $v(z)$. A zero-mean Gaussian white noise vertical acceleration input ($u_y(t)$) has been introduced to simulate the environmental operational excitation to the structural system [37], previously scaled up to $0.01g$ of peak acceleration. Through time history analyses, the vibrational response data have been collected by the FE nodes of the uniform mesh labeled as $1, 2, 3, 4$, and 5, simulating the sensors placement of 5 MEMS accelerometers with a sampling frequency of $500Hz$. The undamaged situation has been set as the reference state, whereas the current damage state may be undamaged (denoted in the following as UD), or with low damage (denoted in the following as LD), i.e. reducing the cross-sectional area of 25%, otherwise with high damage (denoted in the following as HD), i.e. with a severe cross section reduction of 50%. The number of damaged FE elements and their location on the beam domain has been randomly chosen. Vibrational response acquisitions have a duration of five-minute, are performed both on reference and current state models, and have been corrupted by additive Gaussian noise to simulate MEMS-like sensors with three SNR levels, referred to low, medium, and high-quality sensing technology (20dB, 40dB, and 60dB respectively). Controlling the random seed to ensure reproducibility from 1 to 5000, in total 5000 monitoring simulations have been conducted.

5 MLP multi-class damage classification results

The damage detection problem with MEMS-like noisy vibrational data has been formulated as a multi-class classification task between the UD, the LD, and the HD classes [38,39]. Fig.3 illustrates the input data dimensions to feed the MLP neural model for both methods (A) and (B). Given 5 MEMS sensors placed on the beam with 500Hz sampling frequency, the total number n of time steps in each time series is 150000. Since the 5000 simulations were conducted in both reference and current health state of the FE beam model, the six statistical features have been computed for the two states and for every sensor, delivering an input feature vector $\boldsymbol{x}$ of size equal to 60 for each of the 5000 simulations. Method (B) requires computing Yan's et al. DIs [33]. However, to contain the computational cost, it is convenient to find a reasonable range of values considering different

Table 3. Summary of the properties of the implemented MLP

Layer	Output Shape	Activation Function	Parameters Number
Input and reshape layer	[(None,80)]	-	0
Hidden layer	(None,15)	ReLU	930
Output Dense Layer	(None,3)	Softmax	48

Total Trainable parameters: 3773
Trainable parameters:3663
Epochs: 1000
Loss: Categorical Cross-entropy (Optimizer: Adam)

time shift parameters and active subspace dimensions. In contrast to the null subspace, the active one is referred to as the non-zero SV. Focusing on a specific time shift, the Yan et al. indicator value differs among the considered active space dimensions [23]. Therefore, method (B) considers time shifts varying from 5 to 25 and truncation orders, which define active space dimensions, from 1 to 4, collecting in total 80 features for each simulation of the whole 5000 time-history runs.

The MLP classifier has been implemented in Python with the Keras module [40]. Table 3 summarizes the architecture of the MLP, which presents a single hidden layer of 15 units and an output layer of 3 units with softmax activation, thus representing the probability of the input feature vector belonging to each possible damaged class. The loss function is the categorical cross-entropy loss, i.e. widely adopted in multi-class classification tasks, and the adam gradient descent weight optimization algorithm has been used. For both methods (A) and (B), the input vectors dataset has been subdivided into an 80% training set (4000 simulations), with a further partition of 10% of the training acting as a validation set, and an 20% test set (1000 simulations).

The after-training results on the test sets with the various SNR cases and for both the methods (A) and (B) have been reported in the confusion matrices of Table 4 and summarized in Fig.4. The accuracies (Acc. in Table 4), are all above 90% for MLP demonstrating a fairly good noise immunity performance for damage detection needs. The precision (Pre. rows in Table 4) and recall (Rec. columns in Table 4) present also quite high values, being above the 87.69% for all the classification possible outcomes in MLP models. The noticeable classification performance of method (B) to method (A) proves that considering an entire set of informative subspace-based features improves the classification performances of the DL models for the damage detection task and further increases the noise immunity of the MLP model. Furthermore, this demonstrated that for realistic MEMS-like sensors, Yan's et al. DI is still an effective damage-sensitive feature in SHM even with high noise levels. Despite the simple and shallow architecture, the current MLP models provide quite interesting multi-class classification results both considering the statistical time series features or Yan et al. subspace-based DI only. Furthermore, a good generalization of the current DL models is

related to the fact that the 5000 numerical simulations randomly considered both how many damaged elements to consider and the level of damage to associate with those selected elements, covering many different damaged and undamaged current states.

Finally, for the sake of comparisons, the results for the method (A) trained with noise-free data, similarly to [23], have been reported in Table 5. The accuracy level of method (A) with noise-free data is always about 1% lower than the accuracy of method (A) with MEMS-like noisy data, except for the case of 40dB in which it is practically the same value. This behavior may be related to the fact that method (A) relies on statistical indicators only of the time series signals. Thus, with noise introduction, the signal changes influence also the statistical features, providing more varying statistical features, and probably enhancing the training performances of the MLP model. Nevertheless, the results with noisy data represent a more realistic real-world scenario, ensuring also a fairly good

Table 4. MLP confusion matrices for the variable noise cases in method (A) and (B).

A-20dB	*Predicted*			
True	UD	LD	HD	*Rec.*
UD	347 0.3470	0 0.0000	0 0.0000	1.0000
LD	11 0.0110	292 0.2920	15 0.0150	0.9182
HD	11 0.0110	27 0.0270	297 0.2970	0.8866
Pre.	0.9404	0.9154	0.9519	**Acc: 0.9360**

B-20dB	*Predicted*			
True	UD	LD	HD	*Rec.*
UD	352 0.3520	0 0.0000	0 0.0000	1.0000
LD	11 0.0110	315 0.3150	0 0.0000	0.9663
HD	10 0.0100	0 0.0000	312 0.3120	0.9689
Pre.	0.9437	1.0000	1.0000	**Acc: 0.9790**

A-40dB	*Predicted*			
True	UD	LD	HD	*Rec.*
UD	336 0.3360	0 0.0000	0 0.0000	1.0000
LD	12 0.0120	300 0.3000	27 0.0270	0.8850
HD	7 0.0070	33 0.0330	285 0.2850	0.8769
Pre.	0.9465	0.9009	0.9135	**Acc: 0.9210**

B-40dB	*Predicted*			
True	UD	LD	HD	*Rec.*
UD	363 0.3630	0 0.0000	0 0.0000	1.0000
LD	12 0.0120	295 0.2950	0 0.0000	0.9609
HD	11 0.0110	0 0.0000	319 0.3190	0.9667
Pre.	0.9404	1.0000	1.0000	**Acc: 0.9770**

A-60dB	*Predicted*			
True	UD	LD	HD	*Rec.*
UD	367 0.3670	1 0.0010	1 0.0010	0.9946
LD	12 0.0120	304 0.3040	17 0.0170	0.9129
HD	5 0.0050	28 0.0280	265 0.2650	0.8893
Pre.	0.9557	0.9129	0.9364	**Acc: 0.9360**

B-60dB	*Predicted*			
True	UD	LD	HD	*Rec.*
UD	338 0.3380	0 0.0000	0 0.0000	1.0000
LD	7 0.0070	319 0.3190	1 0.0010	0.9755
HD	11 0.0110	1 0.0010	323 0.3230	0.9642
Pre.	0.9494	0.9969	0.9969	**Acc: 0.9800**

Table 5. MLP confusion matrix for the method (A) with noise-free data.

A-Noise-free	*Predicted*			
True	UD	LD	HD	*Rec.*
UD	358 0.3580	0 0.0000	0 0.0000	1.0000
LD	16 0.0160	277 0.2770	22 0.0220	0.8794
HD	5 0.5000	35 0.0350	287 0.2870	0.8777
Pre.	0.9446	0.8878	0.9288	**Acc: 0.9220**

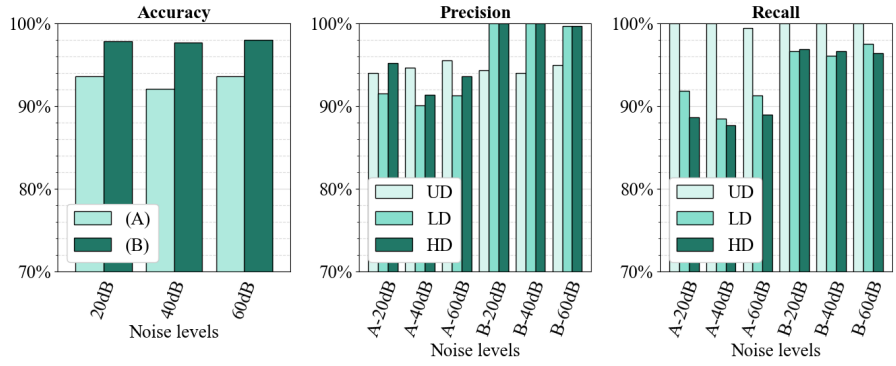

Fig. 4. Overall accuracy, precision and recall for methods (A), (B) and three noise levels.

noise immunity of the trained model for damage identification purposes in the SHM paradigm.

6 Conclusions

In this study, the authors proposed two AI-aided monitoring techniques in presence of noisy output-only vibrational response data. The first method (A) relies on a set of statistical indicators directly computed on the time series vibrational response, whereas the second method has its roots in the OMA SSI-cov method employing the set of Yan's et al. [33] subspace-based damage sensitive features computed between an undamaged reference health state and a current, possibly damaged, state. The damage detection task has been formulated as a multi-class classification task among three possible states (UD, LD, and HD), handled with a shallow MLP network architecture. Both the obtained models were apparently able to recognize the damage levels, additionally presenting a fairly good noise immunity. The analyzed MLP models could represent an interesting and valuable first-level anomaly detection even in real-world noisy cases where the damage scenario is rarely known in advance.

Acknowledgments

This research has been supported by the ADDOPTML (ntua.gr) project: "ADDitively Manufactured OPTimized Structures by means of Machine Learning" (No: 101007595) belonging to the Marie Skłodowska-Curie Actions (MSCA) Research and Innovation Staff Exchange (RISE) H2020-MSCA-RISE-2020. The authors would like to thank G.C. Marano and the project ADDOPTML for funding supporting this research.

References

1. Charles R Farrar and Keith Worden. *Structural health monitoring: a machine learning perspective*. John Wiley & Sons, 2012.
2. Carlo Rainieri and Giovanni Fabbrocino. Operational modal analysis of civil engineering structures. *Springer, New York*, 142:143, 2014.
3. Giuseppe Carlo Marano, Francesco Trentadue, and Floriana Petrone. Optimal arch shape solution under static vertical loads. *Acta Mechanica*, 225(3):679–686, 2014.
4. Giuseppe Carlo Marano and Giuseppe Quaranta. A new possibilistic reliability index definition. *Acta mechanica*, 210(3):291–303, 2010.
5. Evangelia Frangedaki, Laura Sardone, and Nikos D Lagaros. Design optimization of tree-shaped structural systems and sustainable architecture using bamboo and earthen materials. *Journal of Architectural Engineering*, 27(4):04021033, 2021.
6. Amedeo Manuello, Gianni Niccolini, and Alberto Carpinteri. Ae monitoring of a concrete arch road tunnel: Damage evolution and localization. *Engineering Fracture Mechanics*, 210:279–287, 2019.
7. Alberto Carpinteri, Giuseppe Lacidogna, and Amedeo Manuello. Damage mechanisms interpreted by acoustic emission signal analysis. In *Key Engineering Materials*, volume 347, pages 577–582. Trans Tech Publ, 2007.
8. Dag Pasquale Pasca, Angelo Aloisio, Marco Martino Rosso, and Stefanos Sotiropoulos. Pyoma and pyoma_gui: A python module and software for operational modal analysis. *SoftwareX*, 20:101216, 2022.
9. Angelo Aloisio, Elena Antonacci, Massimo Fragiacomo, and Rocco Alaggio. The recorded seismic response of the santa maria di collemaggio basilica to low-intensity earthquakes. *International Journal of Architectural Heritage*, 15(1):229–247, 2021.
10. Angelo Aloisio, Dag Pasquale Pasca, Luca Battista, Marco Martino Rosso, Raffaele Cucuzza, Giuseppe Marano, and Rocco Alaggio. Indirect assessment of concrete resistance from fe model updating and young's modulus estimation of a multi-span psc viaduct: Experimental tests and validation. *Elsevier Structures*, 37:686–697, 01 2022.
11. Amedeo Manuello Bertetto, Davide Masera, and Alberto Carpinteri. Acoustic emission monitoring of the turin cathedral bell tower: Foreshock and aftershock discrimination. *Applied Sciences*, 10(11):3931, 2020.
12. Marco Martino Rosso, Giulia Marasco, Salvatore Aiello, Angelo Aloisio, Bernardino Chiaia, and Giuseppe Carlo Marano. Convolutional networks and transformers for intelligent road tunnel investigations. *Computers & Structures*, 275:106918, 2023.
13. Giuseppe Lacidogna, Amedeo Manuello, Gianni Niccolini, and Alberto Carpinteri. Acoustic emission monitoring of italian historical buildings and the case study of the athena temple in syracuse. *Architectural Science Review*, 58(4):290–299, 2015.
14. Angelo Aloisio, Marco Martino Rosso, and Rocco Alaggio. Experimental and analytical investigation into the effect of ballasted track on the dynamic response of railway bridges under moving loads. *Journal of Bridge Engineering*, 27(10):04022085, 2022.
15. Marco Martino Rosso, Raffaele Cucuzza, Giuseppe Carlo Marano, Angelo Aloisio, and Dag Pasquale Pasca. Indirect estimate of concrete compression strength framework with fe model updating and operational modal analysis. page 1611 – 1618. International Association for Bridge and Structural Engineering (IABSE), 2022. Cited by: 0; Conference name: IABSE Symposium Prague 2022: Challenges for Existing and Oncoming Structures; Conference date: 25 May 2022 through 27 May 2022; Conference code: 180214.

16. Luis David Avendaño-Valencia and Spilios D. Fassois. Gaussian mixture random coefficient model based framework for shm in structures with time–dependent dynamics under uncertainty. *Mechanical Systems and Signal Processing*, 97:59–83, 2017. Special Issue on Surveillance.
17. Rune Brincker and Carlos E. Ventura. *Introduction to Operational Modal Analysis*. John Wiley & Sons, Ltd, 2015.
18. S. Das, P. Saha, and S.K. Patro. Vibration-based damage detection techniques used for health monitoring of structures: a review. *Springer Journal of Civil Structural Health Monitoring*, 6:477–507, 2016.
19. Anders Rytter. *Vibrational Based Inspection of Civil Engineering Structures*, volume Fracture & dynamics Vol. R9314 No. 44. Aalborg University, Dept. of Building Technology and Structural Engineering, 1993. Ph.D. thesis.
20. Ulrike Dackermann, Wade A Smith, Jianchun Li, and Robert B Randall. On the use of the cepstrum and artificial neural networks to identify structural mass changes from response-only measurements. *ISMA, Leuven, Belgium*, pages 15–17, 2014.
21. Minkyu Kim and Junho Song. Near-real-time identification of seismic damage using unsupervised deep neural network. *Journal of Engineering Mechanics*, 148(3):04022006, 2022.
22. Rafaelle Piazzaroli Finotti, Alexandre Abrahão Cury, and Flávio de Souza Barbosa. An shm approach using machine learning and statistical indicators extracted from raw dynamic measurements. *Latin American Journal of Solids and Structures*, 16, 2019.
23. Marco M. Rosso, Angelo Aloisio, Raffaele Cucuzza, Dag P. Pasca, Giansalvo Cirrincione, and Giuseppe C. Marano. Structural health monitoring with artificial neural network and subspace-based damage indicators. In *ISIC 2022, Guimarães, Portugal, September 6-9, 2022 (in press)*, pages 1–14. Springer, 2023.
24. Jyrki Kullaa. Detection, identification, and quantification of sensor fault in a sensor network. *Mechanical Systems and Signal Processing*, 40:208–221, 2013.
25. Jong-Hyun Jeong, Hongki Jo, Simon Laflamme, Jian Li, Austin Downey, Caroline Bennett, William Collins, Sdiq Anwar Taher, Han Liu, and Hyung-Jo Jung. Automatic control of ac bridge-based capacitive strain sensor interface for wireless structural health monitoring. *Measurement*, 202:111789, 2022.
26. A Carpinteri, G Lacidogna, A Manuello, and G Niccolini. Acoustic emission wireless transmission system for structural and infrastructural networks. In *8th Internation Conference on Fracture Mechanics of Concrete and Concrete Strucures*, 2013.
27. Shang Gao, Xuewu Dai, Zheng Liu, Guiyun Tian, and Shenfang Yuan. A wireless piezoelectric sensor network for distributed structural health monitoring. pages 1–6, 2015.
28. Li Zhu, Yuguang Fu, Raymond Chow, Billie F. Spencer, Jongwoong Park, and Kirill Mechitov. Development of a high-sensitivity wireless accelerometer for structural health monitoring. *Sensors (Basel, Switzerland)*, 18, 2018.
29. Ashiqur Rahaman, Chung Hyuk Park, and Byungki Kim. Design and characterization of a mems piezoelectric acoustic sensor with the enhanced signal-to-noise ratio. *Sensors and Actuators A: Physical*, 311:112087, 2020.
30. Y.C. He, Z. Li, J.Y. Fu, J.R. Wu, and C.T. Ng. Enhancing the performance of stochastic subspace identification method via energy-oriented categorization of modal components. *Engineering Structures*, 233:111917, 2021.

31. Knut Andreas Kvåle, Ole Øiseth, and Anders Rønnquist. Operational modal analysis of an end-supported pontoon bridge. *Engineering Structures*, 148:410–423, 2017.
32. Michèle Basseville, Maher Abdelghani, and Albert Benveniste. Subspace-based fault detection algorithms for vibration monitoring. *Autom.*, 36:101–109, 2000.
33. Ai-Min Yan and Jean-Claude Golinval. Null subspace-based damage detection of structures using vibration measurements. *Mechanical Systems and Signal Processing*, 20(3):611–626, 2006.
34. Minjie Zhu, Frank McKenna, and Michael H Scott. Openseespy: Python library for the opensees finite element framework. *SoftwareX*, 7:6–11, 2018.
35. Jonathan Melchiorre, Amadeo Manuello, Laura Sardone, and Giuseppe Carlo Marano. Damaging configurations in arch structures with variable curvature and tapered cross-section. *WCCM-APCOM 2022*, 900, 2022.
36. J Melchiorre, A Manuello, F Marmo, S Adriaenssens, and GC Marano. Differential formulation and numerical solution for elastic arches with variable curvature and tapered cross-sections. *European Journal of Mechanics-A/Solids*, 97:104757, 2023.
37. Eduardo Becker Groth, Thomas Gabriel Rosauro Clarke, Guilherme Schumacher da Silva, Ignacio Iturrioz, and Giuseppe Lacidogna. The elastic wave propagation in rectangular waveguide structure: Determination of dispersion curves and their application in nondestructive techniques. *Applied Sciences*, 10(12), 2020.
38. Meghdad Khazaee, Pierre Derian, and Anthony Mouraud. A comprehensive study on structural health monitoring (shm) of wind turbine blades by instrumenting tower using machine learning methods. *Renewable Energy*, 199:1568–1579, 2022.
39. Xuyan Tan, Weizhong Chen, Tao Zou, Jianping Yang, and Bowen Du. Real-time prediction of mechanical behaviors of underwater shield tunnel structure using machine learning method based on structural health monitoring data. *Journal of Rock Mechanics and Geotechnical Engineering*, 2022.
40. Francois Chollet et al. Keras, 2015.